PROCEEDINGS OF SCIENCE

Open Charm decays and spectroscopy at Belle

arXiv:1611.04253v1 [hep-ex] 14 Nov 2016

B. Pal, A. Schwartz[*†]
University of Cincinnati
E-mail: palbs@ucmail.uc.edu

In this review we report the recent results of open charm decays and spectroscopy using the data collected with the Belle detector at the KEKB asymmetric-energy e^+e^- collider.

VIII International Workshop on Charm Physics
5-9 September, 2016
Bologna, ITALY

[*]Speaker.
[†]On behalf of the Belle Collaboration

© Copyright owned by the author(s) under the terms of the Creative Commons Attribution-NonCommercial-NoDerivatives 4.0 International License (CC BY-NC-ND 4.0).

1. Introduction

In this report an overview of the recent results of open charm decays and spectroscopy is presented based on the data, collected by the Belle experiment at the KEKB e^+e^- asymmetric-energy collider [1]. (Throughout this paper charge-conjugate modes are implied.) The experiment took data at center-of-mass energies corresponding to several $\Upsilon(nS)$ resonances; the total data sample recorded exceeds 1 ab^{-1}.

The Belle detector is a large-solid-angle magnetic spectrometer that consists of a silicon vertex detector (SVD), a 50-layer central drift chamber (CDC), an array of aerogel threshold Cherenkov counters (ACC), a barrel-like arrangement of time-of-flight scintillation counters (TOF), and an electromagnetic calorimeter comprised of CsI(Tl) crystals (ECL) located inside a super-conducting solenoid coil that provides a 1.5 T magnetic field. An iron flux-return located outside of the coil is instrumented to detect K_L^0 mesons and to identify muons (KLM). The detector is described in detail elsewhere [2, 3].

2. Analysis of D^{**} production

Orbitally excited states of the D meson (D^{**} states) provide a good opportunity to test the heavy quark effective theory (HQET) [4] and QCD sum rule [5] predictions. Precise knowledge of the properties of the D^{**} state is important to reduce uncertainties in the measurements of the semileptonic decays and thus in the determination of the Cabibbo-Kobayashi-Maskawa matrix elements $|V_{cb}|$ and $|V_{ub}|$. Many D^{**} mesons have already been observed by B factories and LHCb [6]. In this analysis, we perform an amplitude analysis of the $\bar{B}^0 \to D^{*+}\omega\pi^-$ decay to measure the decay fractions of D^{**} states and to study the D^{**} properties [7], using 711 fb^{-1} of data collected at the $\Upsilon(4S)$ resonance.

The total signal yield is obtained from a binned χ^2 fit to the $\Delta E = \sqrt{|\vec{p}|^2 + m^2} - E_{\rm beam}$ distribution, with a tight cut in the beam-constrained mass $M_{\rm bc}$. The corresponding branching fraction is measured to be

$$\mathscr{B}(\bar{B}^0 \to D^{*+}\omega\pi^-) = (2.31 \pm 0.11 \pm 0.14) \times 10^{-3}.$$

Unless explicitly stated otherwise, whenever two uncertainties are quoted in this proceeding, the first is statistical and the second is systematic. The result is consistent with the values of CLEO [8] and BaBar [9] but with higher precision.

A six-dimensional amplitude analysis is performed using the method described in Ref. [10]. We define two sets of variables: [$M^2(\omega\pi)$, $\cos\theta_1$, ϕ_1, $\cos\beta_1$, ψ_1, $\cos\xi_1$] and [$M^2(D^*\pi)$, $\cos\theta_2$, ϕ_2, $\cos\beta_2$, ψ_2, $\cos\xi_2$], corresponding to the $\omega\pi$ and D^{**} production, respectively. The masses $M(\omega\pi)$ and $M(D^*\pi)$ are the invariant masses of the $\omega\pi$ and $D^*\pi$ combinations. The angular variables describing $\omega\pi$ production are defined in Fig. 1. The angular variables describing D^{**} production are defined in the same manner as angles for $\omega\pi$ production, but with the $D^*\pi$ flight direction instead of the $\omega\pi$.

To describe all the features of the Dalitz plot, we use the following set of resonances: off-shell $\rho(770)^-$, $\rho(1450)^-$, $D_1(2430)^0$, $D_1(2420)^0$, $D_2^*(2460)^0$ and $b_1(1235)^-$. Figure 2 shows the projections of $M^2(\omega\pi)$ and $M^2(D^*\pi)$ distributions and the results are summarized in Table 1.

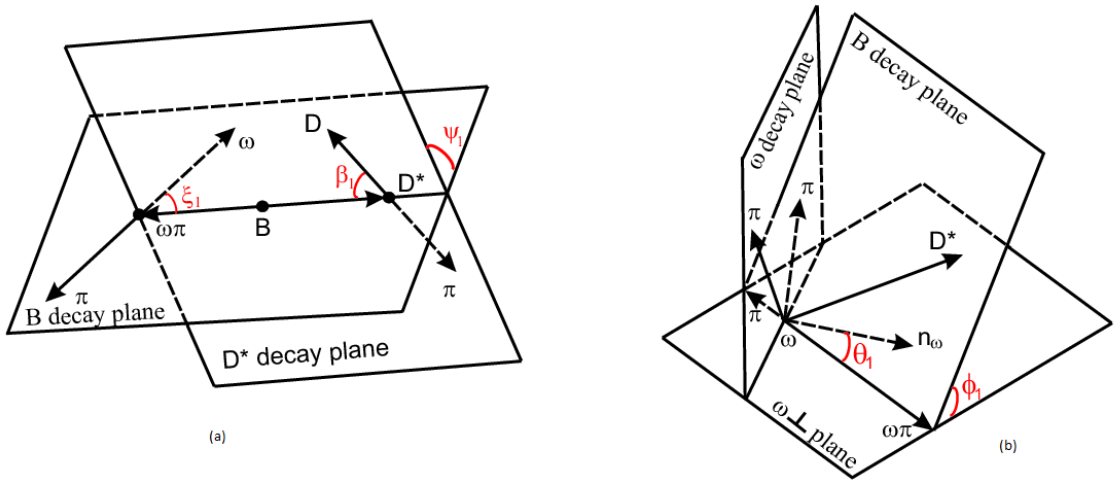

Figure 1: Kinematics of a $\bar{B}^0 \to D^{*+}\omega\pi^-$ decay mediated by an $\omega\pi^-$ intermediate resonance. The diagram in (a) defines two polar angles ξ_1 and β_1 and one azimuthal angle ψ_1. The diagram in (b) defines one polar angle θ_1 and one azimuthal angle ϕ_1. The direction n_ω in (b) corresponds to the vector normal to the ω decay plane.

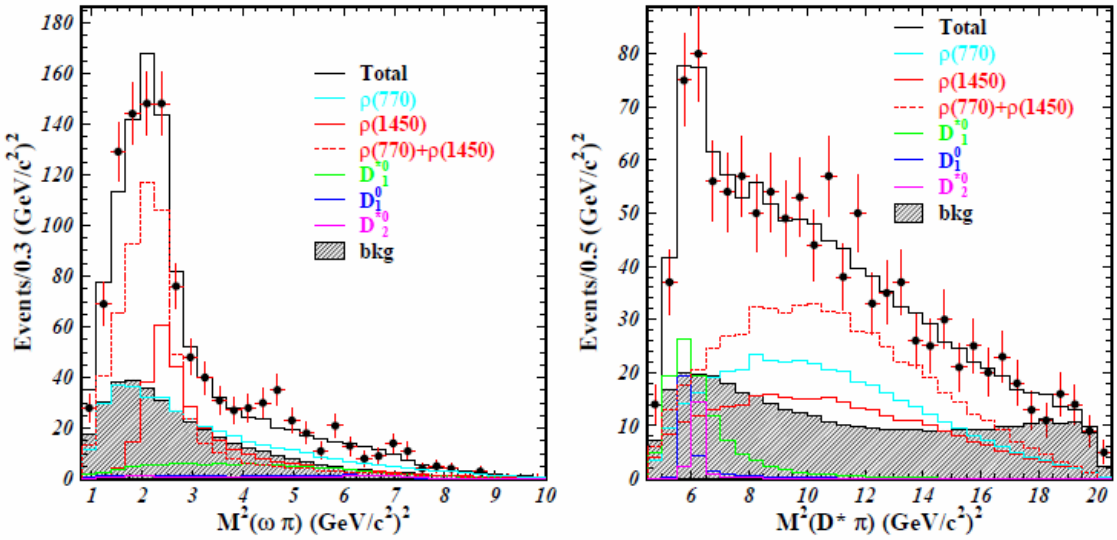

Figure 2: Distributions of the variables (left) $M^2(\omega\pi)$ and (right) $M^2(D^*\pi)$.

3. Analysis of charmed baryon decays

3.1 First observation of the doubly Cabibbo-suppressed Λ_c^+ decay

Several doubly Cabibbo-suppressed (DCS) decays of charmed mesons have been observed [6]. Their measured branching ratios with respect to the corresponding Cabibbo-favored (CF) decays play an important role in constraining models of the decay of charmed hadrons and in the study of flavor- $SU(3)$ symmetry [11, 12]. On the other hand, because of the smaller production cross sec-

Table 1: Summary of the final results of the $\bar{B}^0 \to D^{*+}\omega\pi^-$ amplitude analysis. The first error is statistical, the second is systematic and the third is the model error.

Parameter	Result
$\mathscr{B}(\bar{B}^0 \to \rho(770)^- D^{*+})$	$(1.48 \pm 0.27^{+0.15+0.21}_{-0.09-0.56}) \times 10^{-3}$
$\mathscr{B}(\bar{B}^0 \to \rho(1450)^- D^{*+})$	$(1.07^{+0.15+0.06+0.40}_{-0.31-0.13-0.02}) \times 10^{-3}$
Mass of $\rho(1450)^-$	$(1544 \pm 22^{+11+1}_{-\ 1-46})$ MeV/c^2
Width of $\rho(1450)^-$	$(303^{+31+3+69}_{-52-4-\ 6})$ MeV
$\mathscr{B}(\bar{B}^0 \to D_1(2430)^0\omega)$	$(2.5 \pm 0.4^{+0.7+0.4}_{-0.2-0.1}) \times 10^{-4}$
S-wave fraction	$(38.9 \pm 10.8^{+4.3+1.2}_{-0.7-1.1})\%$
P-wave fraction	$(33.1 \pm 9.5^{+2.4+3.0}_{-5.5-4.0})\%$
D-wave fraction	$(28.3 \pm 8.9^{+3.0+3.9}_{-0.8-2.9})\%$
Longitudinal polarization	$(63.0 \pm 9.1 \pm 4.6^{+4.6}_{-3.9})\%$
$\mathscr{B}(\bar{B}^0 \to D_1(2420)^0\omega)$	$(0.7 \pm 0.2^{+0.1}_{-0.0} \pm 0.1) \times 10^{-4}$
Longitudinal polarization	$(67.1 \pm 11.7^{+0.0+2.3}_{-4.2-2.8})\%$
$\mathscr{B}(\bar{B}^0 \to D_2^*(2460)^0\omega)$	$(0.4 \pm 0.1^{+0.0}_{-0.1} \pm 0.1) \times 10^{-4}$
Longitudinal polarization	$(76.0^{+18.3}_{-8.5} \pm 2.0^{+2.9}_{-2.0})\%$
$\mathscr{B}(\bar{B}^0 \to b_1(1235)^- D^{*+})$	$< 0.7 \times 10^{-4}$ at 90% confidence level

tions for charmed baryons, DCS decays of charmed baryons have not yet been observed. Here we present the first observation of the DCS decay $\Lambda_c^+ \to pK^+\pi^-$ and the measurement of its branching ratio with respect to the CF decay $\Lambda_c^+ \to pK^-\pi^+$, using 980 fb^{-1} of data [13].

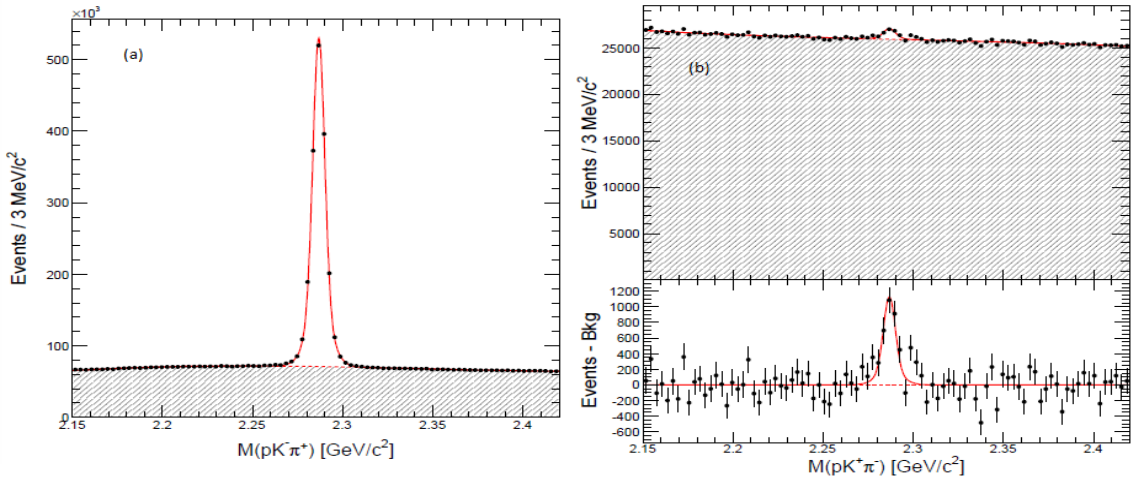

Figure 3: Distributions of (a) $M(pK^-\pi^+)$ and (b) $M(pK^+\pi^-)$ and residuals of data with respect to the fitted combinatorial background. The solid curves indicate the full fit model and the dashed curves the combinatorial background.

Figure 3 shows invariant mass distributions of (a) $pK^-\pi^+$ (CF) and (b) $pK^+\pi^-$ (DCS) combinations. DCS decay events are clearly observed in $M(pK^+\pi^-)$. In order to obtain the signal yield, a binned least-χ^2 fit is performed. From the mass fit, we extract $(1.452 \pm 0.015) \times 10^6$ $\Lambda_c^+ \to pK^-\pi^+$ events and 3587 ± 380 $\Lambda_c^+ \to pK^+\pi^-$ events. The latter has a peaking background from the single Cabibbo-suppressed (SCS) decay $\Lambda_c^+ \to \Lambda(\to p\pi^-)K^+$, which has the same final-state topology. After subtracting the SCS contribution, we have $3379 \pm 380 \pm 78$ DCS events, where the first uncertainty is statistical and the second is the systematic due to SCS subtraction. The corresponding statistical significance is 9.4 standard deviations. We measure the branching ratio, $\frac{\mathscr{B}(\Lambda_c^+ \to pK^+\pi^-)}{\mathscr{B}(\Lambda_c^+ \to pK^-\pi^+)} = (2.35 \pm 0.27 \pm 0.21) \times 10^{-3}$, and the absolute branching fraction of the DCS decay, $\mathscr{B}(\Lambda_c^+ \to pK^+\pi^-) = (1.61 \pm 0.23^{+0.07}_{-0.08}) \times 10^{-4}$. This measured branching ratio corresponds to $(0.82 \pm 0.21) \tan^4\theta_c$, where the uncertainty is the total, which suggests a slightly smaller decay width than the naïve expectation [14]. After subtracting the contributions of $\Lambda^*(1520)$ and Δ isobar intermediates, which contribute only to the CF decay, the revised ratio, $\frac{\mathscr{B}(\Lambda_c^+ \to pK^+\pi^-)}{\mathscr{B}(\Lambda_c^+ \to pK^-\pi^+)} = (1.10 \pm 0.17) \tan^4\theta_c$ is consistent with the naïve expectation.

3.2 Study of excited Ξ_c states decaying into Ξ_c^0 and Ξ_c^+ baryons

We present measurements of the masses of all members of the Ξ_c', $\Xi_c(2645)$, $\Xi_c(2790)$, $\Xi_c(2815)$ and $\Xi_c(2980)$ isodoublets, measurements of the intrinsic widths of those that decay strongly, and evidence of previously unknown transitions [15]. This analysis is based on 980 fb^{-1} of data. The following decay chains are used: $\Xi_c(2980) \to \Xi_c(2645)\pi \to \Xi_c\pi\pi$, $\Xi_c(2980) \to \Xi_c'\pi \to \Xi_c\gamma\pi$, $\Xi_c(2815) \to \Xi_c(2645)\pi \to \Xi_c\pi\pi$, $\Xi_c(2815) \to \Xi_c'\pi \to \Xi_c\gamma\pi$ and $\Xi_c(2790) \to \Xi_c'\pi \to \Xi_c\gamma\pi$. To obtain large statistics, we use many decay modes of the ground-state Ξ_c^0 and Ξ_c^+ baryons.

Table 2 shows the results of the measurements of masses and widths of the five isodoublets. Of the eighteen measurements, five are of intrinsic widths of particles for which only limits existed previously. Of the remaining thirteen measurements, ten are within one standard deviation of the Particle Data Group [6] best-fit values. The three measurements that are in modest disagreement with previous results are in the $\Xi_c(2980)$ sector, where the previous measurements were dominated by decays into different final states and for which some measurements may have been prone to the existence of more than one resonance in the region, or biases from threshold effects. Measurements of the isospin splittings, give in Table 3 are in good agreement with predictions of non-relativistic quark model [16].

3.3 Studies of charmed strange baryons in the ΛD final state

To date, all measurements of the excited Ξ_c were performed using decays in which the charm quark is contained in the final state baryon. Measurements of final states in which the charm quark is part of the final state meson provide complementary information. Here we present the studies of Ξ_c^* baryons decaying to ΛD^+ and ΛD^0 final states using 980 fb^{-1} of data [17].

Figures 4 (a) show the fit to the ΛD^+ invariant mass distribution. Peaks of $\Xi_c(3055)^+$ and $\Xi_c(3080)^+$ states with statistical significances of 11.7 and 4.8 standard deviations, respectively are seen in the ΛD^+ final state. These correspond to first observation of $\Xi_c(3055)^+ \to \Lambda D^+$ and first evidence of $\Xi_c(3080)^+ \to \Lambda D^+$ decays. The mass and width of the $\Xi_c(3055)^+$ are obtained to be $(3055.8 \pm 0.4 \pm 0.2)$ MeV/c^2 and $(7.0 \pm 1.2 \pm 1.5)$ MeV, respectively, and those for $\Xi_c(3080)^+$ are

Table 2: The results of the measurements of masses (in MeV/c^2) and widths (in MeV) of the five isodoublets. In all cases, the first uncertainty is statistical, and the second is the systematic uncertainty associated with the individual measurement. All the masses have a final, asymmetric uncertainty, taken from the Particle Data Group [6], for the mass of the ground states, and the $\Xi_c(2790)$ have an extra uncertainty due to the uncertainty in the $M(\Xi_c') - M(\Xi_c)$ measurement.

Particle	Mass	Width
$\Xi_c(2645)^+$	$2645.58 \pm 0.06 \pm 0.07^{+0.28}_{-0.40}$	$2.06 \pm 0.13 \pm 0.13$
$\Xi_c(2645)^0$	$2646.43 \pm 0.07 \pm 0.07^{+0.28}_{-0.40}$	$2.35 \pm 0.18 \pm 0.13$
$\Xi_c(2815)^+$	$2816.73 \pm 0.08 \pm 0.06^{+0.28}_{-0.40}$	$2.43 \pm 0.20 \pm 0.17$
$\Xi_c(2815)^0$	$2820.20 \pm 0.08 \pm 0.07^{+0.28}_{-0.40}$	$2.54 \pm 0.18 \pm 0.17$
$\Xi_c(2980)^+$	$2966.0 \pm 0.8 \pm 0.2^{+0.3}_{-0.4}$	$28.1 \pm 2.4^{+1.0}_{-5.0}$
$\Xi_c(2980)^0$	$2970.8 \pm 0.7 \pm 0.2^{+0.3}_{-0.4}$	$30.3 \pm 2.3^{+1.0}_{-1.8}$
$\Xi_c'^+$	$2578.4 \pm 0.1 \pm 0.4^{+0.3}_{-0.4}$	
$\Xi_c'^0$	$2579.2 \pm 0.1 \pm 0.4^{+0.3}_{-0.4}$	
$\Xi_c(2790)^+$	$2791.6 \pm 0.2 \pm 0.1 \pm 0.4^{+0.3}_{-0.4}$	$8.9 \pm 0.6 \pm 0.8$
$\Xi_c(2790)^0$	$2794.9 \pm 0.3 \pm 0.1 \pm 0.4^{+0.3}_{-0.4}$	$10.0 \pm 0.7 \pm 0.8$

Table 3: Isospin splitting between the members of each isodoublet.

Particle	$M(\Xi_c^+) - M(\Xi_c^0)$ (MeV/c^2)
$\Xi_c(2645)$	$-0.85 \pm 0.09 \pm 0.08 \pm 0.48$
$\Xi_c(2815)$	$-3.47 \pm 0.12 \pm 0.05 \pm 0.48$
$\Xi_c(2980)$	$-4.8 \pm 0.1 \pm 0.2 \pm 0.5$
Ξ_c'	$-0.8 \pm 0.1 \pm 0.1 \pm 0.5$
$\Xi_c(2790)$	$-3.3 \pm 0.4 \pm 0.1 \pm 0.5$

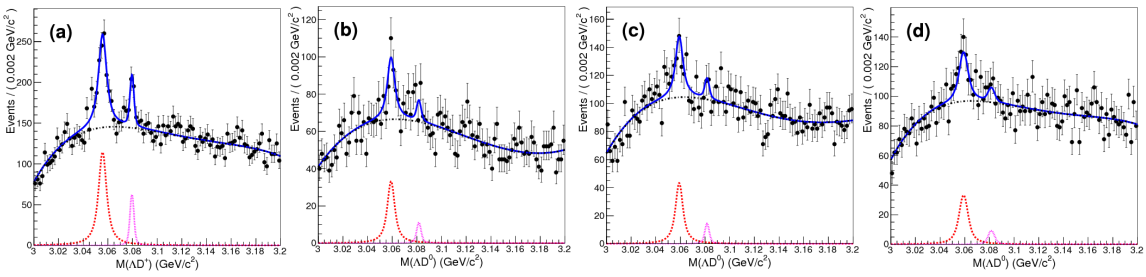

Figure 4: Distributions of (a) $M(\Lambda D^+)$ and (b, c, d) $M(\Lambda D^0)$ for (b) $D^0 \to K^-\pi^+$, (c) $D^0 \to K^-\pi^+\pi^+\pi^-$ and (d) $D^0 \to K^-\pi^+\pi^0$. Points with statistical error bars are data. Blue solid lines show the fit results. The red dashed, magenta dotted, and black dashed-dotted lines show the $\Xi_c(3055)$ signal, the $\Xi_c(3080)$ signal, and the background components, respectively.

$(3079.6 \pm 0.4 \pm 0.1)$ MeV$/c^2$ and < 6.3 MeV at 90% confidence level, respectively. The measured values for $\Xi_c(3055)^+$ are more accurate than the current world average values. Figure 4 (b, c, d) shows the simultaneous fit to the three different D^0 decay modes of ΛD^0 final state. We observe a clear peak of $\Xi_c(3055)^0$ state with a statistical significance of 8.6 standard deviations. The peak for the $\Xi_c(3080)^0$ is not statistically significant. The mass and width of $\Xi_c(3055)^0$ are measured to be $(3059.0 \pm 0.5 \pm 0.6)$ MeV$/c^2$ and $(6.4 \pm 2.1 \pm 1.1)$ MeV, respectively. This is the first observation of the decay $\Xi_c(3055)^0 \to \Lambda D^0$.

We perform a combined analysis of the $\Xi_c(3055)^+$ and $\Xi_c(3080)^+$ by comparing their decays into ΛD^+ with those into $\Sigma_c^{++} K^-$ and $\Sigma_c^{*++} K^-$ final states. We measure the ratios of branching fractions $\frac{\mathscr{B}(\Xi_c(3055)^+ \to \Lambda D^+)}{\mathscr{B}(\Xi_c(3055)^+ \to \Sigma_c^{++} K^-)} = 5.09 \pm 1.01 \pm 0.76$, $\frac{\mathscr{B}(\Xi_c(3080)^+ \to \Lambda D^+)}{\mathscr{B}(\Xi_c(3080)^+ \to \Sigma_c^{++} K^-)} = 1.29 \pm 0.30 \pm 0.15$ and $\frac{\mathscr{B}(\Xi_c(3080)^+ \to \Sigma^{*++} K^-)}{\mathscr{B}(\Xi_c(3080)^+ \to \Sigma_c^{++} K^-)} = 1.07 \pm 0.27 \pm 0.04$. These measurements are in contradictions with the chiral quark model predictions [18]. Further experimental and theoretical work is needed to understand the nature of these baryons. From the combined analysis we measure the widths of the state $\Xi_c(3055)^+$ is $(7.8 \pm 1.2 \pm 1.5)$ MeV and that of $\Xi_c(3080)^+$ is $(3.0 \pm 0.7 \pm 0.4)$ MeV.

4. Analysis of charmed meson decays

4.1 $D^0 \to V\gamma$

The radiative decays $D^0 \to V\gamma$, where V $(\phi, \bar{K}^{*0}, \rho^0)$ is a vector meson, are dominated by long-range contribution. They could be sensitive to NP via *CP* asymmetry [19, 20]. We present here the results of the measurement of the branching fractions and *CP* asymmetries in these decays based on 943 fb^{-1} of data [21]. The candidate D^0 mesons are required to originate from the decay $D^{*+} \to D^0 \pi_S^+$ in order to identify the flavour of the D^0 and to suppress combinatorial background. The signal decays are reconstructed in the following sub-decay channels of the vector meson: $\phi \to K^+K^-$, $\bar{K}^{*0} \to K^-\pi^+$ and $\rho^0 \to \pi^+\pi^-$. The selection criteria are optimized to maximize the figure of merit $N_{\rm sig}/\sqrt{N_{\rm sig}+N_{\rm bkg}}$, where $N_{\rm sig}$ and $N_{\rm bkg}$ represent the number of signal and background events. Both the branching fractions $\mathscr{B}(D^0 \to V\gamma)$ and *CP* asymmetries $\mathscr{A}_{CP}(D^0 \to V\gamma)$ are obtained via normalization to other decay channels. The signal branching fraction $\mathscr{B}_{\rm sig}$ is given by

$$\mathscr{B}_{\rm sig} = \mathscr{B}_{\rm norm} \times \frac{N_{\rm sig}}{N_{\rm norm}} \times \frac{\varepsilon_{\rm norm}}{\varepsilon_{\rm sig}}, \tag{4.1}$$

where N is the extracted yield, ε the reconstruction efficiency and $\mathscr{B}$ the branching fraction for the corresponding mode. For $\mathscr{B}_{\rm norm}$ the world average value [6] is used. We use the decays $D^0 \to K^+K^-$, $D^0 \to K^-\pi^+$ and $D^0 \to \pi^+\pi^-$ as the normalization channels for ϕ, $\bar{K}^{*0}$ and ρ^0 signal modes, respectively. The measured branching fractions are

$$\begin{aligned}
\mathscr{B}(D^0 \to \phi\gamma) &= (2.76 \pm 0.19 \pm 0.10) \times 10^{-5}, \\
\mathscr{B}(D^0 \to \bar{K}^{*0}\gamma) &= (4.66 \pm 0.21 \pm 0.21) \times 10^{-4}, \\
\mathscr{B}(D^0 \to \rho^0\gamma) &= (1.77 \pm 0.30 \pm 0.07) \times 10^{-5}.
\end{aligned}$$

The result of the ϕ mode is improved compared to the previous Belle result [22] and is consistent with the world average value [6]. Our branching fraction for the $\bar{K}^{*0}$ mode is 3.3 σ higher than the BaBar result $\mathscr{B}(D^0 \to \bar{K}^{*0}\gamma) = (3.22 \pm 0.20 \pm 0.27) \times 10^{-4}$ [23]. For the ρ^0 mode, we report the

first observation of the decay with a significance of 5 σ including the systematic uncertainties. The fit results are shown in Fig. 5.

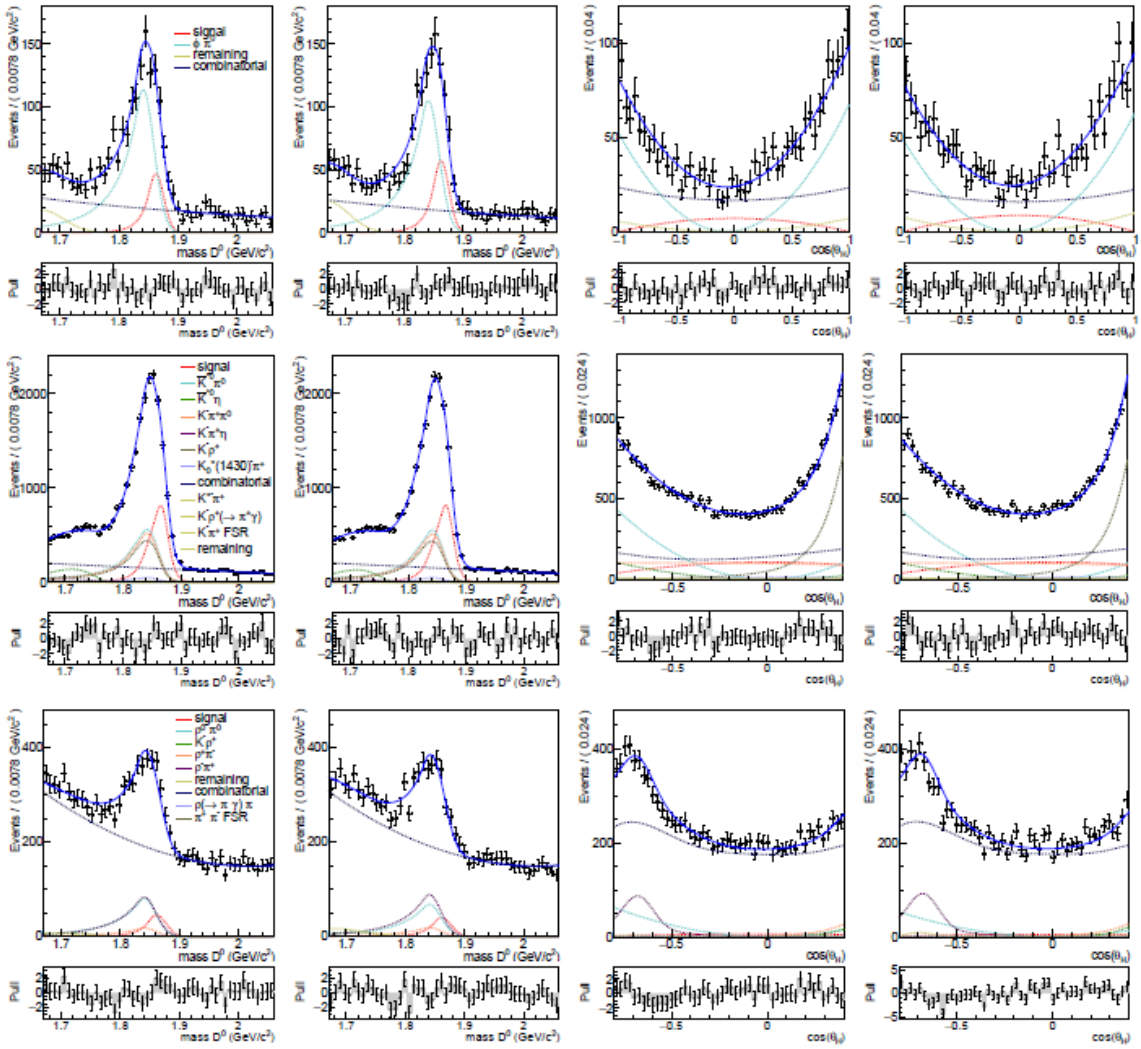

Figure 5: Distributions of the invariant masses and the cosine of the helicity angles of (left) $D^0 \to V\gamma$ and (right) $\bar{D}^0 \to V\gamma$. Top row corresponds to ϕ mode, middle row the $\bar{K}^{*0}$ and the bottom row the ρ^0 mode.

The raw asymmetry is extracted using

$$A_{\rm raw} = \frac{N(D^0) - N(\bar{D}^0)}{N(D^0) + N(\bar{D}^0)}, \tag{4.2}$$

and has several contributions: $A_{\rm raw} = \mathscr{A}_{CP} + A_{\rm FB} + A_\varepsilon^\pm$. The forward-backward production asymmetry $A_{\rm FB}$ and the asymmetry due to different reconstruction efficiencies for pasitively and negatively chraged particles $A_\varepsilon^\pm$ can be eliminated through a relative measurement of $\mathscr{A}_{CP}$, if the charged final state particles are identical. It then follows

$$\mathscr{A}_{CP}^{\rm sig} = A_{\rm raw}^{\rm sig} - A_{\rm raw}^{\rm norm} + \mathscr{A}_{CP}^{\rm norm}, \tag{4.3}$$

where $\mathscr{A}_{CP}^{\rm norm}$ is the nominal value of CP asymmetry [6] of the normalization mode. We measure

$$\begin{aligned}\mathscr{A}_{CP}(D^0 \to \phi\gamma) &= -(0.094 \pm 0.066 \pm 0.001),\\ \mathscr{A}_{CP}(D^0 \to \bar{K}^{*0}\gamma) &= -(0.003 \pm 0.020 \pm 0.000),\\ \mathscr{A}_{CP}(D^0 \to \rho^0\gamma) &= \quad 0.056 \pm 0.152 \pm 0.006.\end{aligned}$$

These are the first-ever $\mathscr{A}_{CP}$ measurements for these decays and are consistent with no CP asymmetry in these modes.

4.2 $D^0 \to K^0_S K^0_S$

In this analysis, we report the preliminary result of a measurement of CP asymmetry in $D^0 \to K^0_S K^0_S$ decays, using 921 fb^{-1} of data [24]. The CP asymmetry of the signal decay mode is given by

$$\mathscr{A}_{CP}^{\rm sig} = A_{\rm raw}^{\rm sig} - A_{\rm raw}^{\rm norm} + \mathscr{A}_{CP}^{\rm norm} + A_{\varepsilon}^{K}. \tag{4.4}$$

The decay $D^0 \to K^0_S\pi^0$ is used as the normalization mode. Here A_{ε}^{K} is the asymmetry due to strong interaction of K^0 and $\bar{K}^0$ mesons with nucleons of the detector material. A simultaneous fit of the

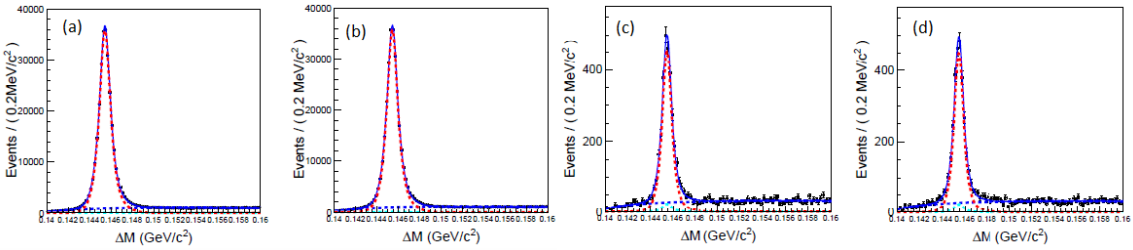

Figure 6: Distributions of ΔM for the $K^0_S\pi^0$ [(a) and (b)] and $K^0_S K^0_S$ [(c) and (d)] final states. (a) and (c) for D^{*+} decays and (b) and (d) for D^{*-} decays. Here points with error bars are the data, the solid curves represent the total fit, dashed blue, cyan and red curves show the non-peaking background, peaking background and signal, respectively.

ΔM for D^{*+} and D^{*-} is used to measure the raw asymmetry, shown in Fig. 6. We measure

$$\mathscr{A}_{CP}(D^0 \to K^0_S K^0_S) = -(0.02 \pm 1.53 \pm 0.17)\%.$$

The result is consistent with no CP violation and with SM expectations [25, 26] and is a significant improvement compared to the previous measurements by CLEO [27] and LHCb [28].

Acknowledgements

The authors thank the workshop organizers for hosting a fruitful and stimulating workshop and providing excellent hospitality. This research is supported by the U.S. Department of Energy.

References

[1] S. Kurokawa and E. Kikutani, Nucl. Instrum. Methods Phys. Res. Sect. A **499**, 1 (2003), and other papers included in this Volume; T.Abe *et al.*, Prog. Theor. Exp. Phys. **2013**, 03A011 (2013) and references therein.

[2] A. Abashian *et al.* (Belle Collaboration), Nucl. Instrum. Methods Phys. Res., Sect. A **479**, 117 (2002); also see the detector section in J.Brodzicka *et al.*, Prog. Theor. Exp. Phys. **2012**, 04D001 (2012).

[3] Z. Natkaniec *et al.* (Belle SVD2 Group), Nucl. Instrum. Methods Phys. Res., Sect. A **560**, 1 (2006).

[4] M. Neubert, Phys. Rept. **245**, 259 (1994).

[5] N. Uraltsev, Phys. Lett. B **501**, 86 (2001).

[6] K. A. Olive *et al.* (Particle Data Group), Chin. Phys. C **38**, 090001 (2014).

[7] D. Matvienko *et al.* (Belle Collaboration), Phys. Rev. D **92**, no. 1, 012013 (2015).

[8] J. P. Alexander *et al.* (CLEO Collaboration), Phys. Rev. D **64**, 092001 (2001).

[9] B. Aubert *et al.* (BaBar Collaboration), Phys. Rev. D **74**, 012001 (2006).

[10] D. V. Matvienko, A. S. Kuzmin and S. I. Eidelman, JHEP **1109**, 129 (2011).

[11] H. J. Lipkin, Nucl. Phys. Proc. Suppl. **115**, 117 (2003).

[12] D. N. Gao, Phys. Lett. B **645**, 59 (2007).

[13] S. B. Yang *et al.* (Belle Collaboration), Phys. Rev. Lett. **117**, 011801 (2016).

[14] J. M. Link *et al.* (FOCUS Collaboration), Phys. Lett. B **624**, 166 (2005).

[15] J. Yelton *et al.* (Belle Collaboration), Phys. Rev. D **94**, 052011 (2016).

[16] B. Silvestre-Brac, F. Brau and C. Semay, J. Phys. G **29**, 2685 (2003).

[17] Y. Kato *et al.* (Belle Collaboration), Phys. Rev. D **94**, 032002 (2016).

[18] L. H. Liu, L. Y. Xiao and X. H. Zhong, Phys. Rev. D **86**, 034024 (2012).

[19] G. Isidori and J. F. Kamenik, Phys. Rev. Lett. **109**, 171801 (2012).

[20] J. Lyon and R. Zwicky, arXiv:1210.6546 [hep-ph].

[21] T. Nanut *et al.* (Belle Collaboration), arXiv:1603.03257 [hep-ex].

[22] K. Abe *et al.* (Belle Collaboration), Phys. Rev. Lett. **92**, 101803 (2004).

[23] B. Aubert *et al.* (BaBar Collaboration), Phys. Rev. D **78**, 071101 (2008).

[24] A. Abdesselam *et al.* (Belle Collaboration), arXiv:1609.06393 [hep-ex].

[25] G. Hiller, M. Jung and S. Schacht, Phys. Rev. D **87**, 014024 (2013).

[26] U. Nierste and S. Schacht, Phys. Rev. D **92**, 054036 (2015).

[27] G. Bonvicini *et al.* (CLEO Collaboration), Phys. Rev. D **63**, 071101 (2001).

[28] R. Aaij *et al.* (LHCb Collaboration), JHEP **1510**, 055 (2015).